Degradation of nanoplastics in the environment: Reactivity and impact on atmospheric and surface waters

Degradation of nanoplastics in the environment: reactivity and impact on atmospheric and surface waters

Angelica Bianco[1], Fabrizio Sordello[2], Mikael Ehn[1], Davide Vione[2], Monica Passananti[1,2,*]

[1] Institute for Atmospheric and Earth System Research/Physics, Faculty of Science, University of Helsinki, FI-00014, Finland.

[2] Dipartimento di Chimica, Università di Torino, Via Pietro Giuria 5, 10125, Torino, Italy.

[*] Corresponding author

E-mail address: monica.passananti@unito.it (M. Passananti)

HIGHLIGHTS

- Smaller nanoplastics particles show higher reactivity with ·OH.
- Reactivity constants of polystyrene nanoparticles with ·OH are measured.
- There is potential for nanoplastics to significantly scavenge ·OH in the environment.
- Degradation of nanoplastics releases organic compounds in the aqueous phase.

GRAPHICAL ABSTRACT

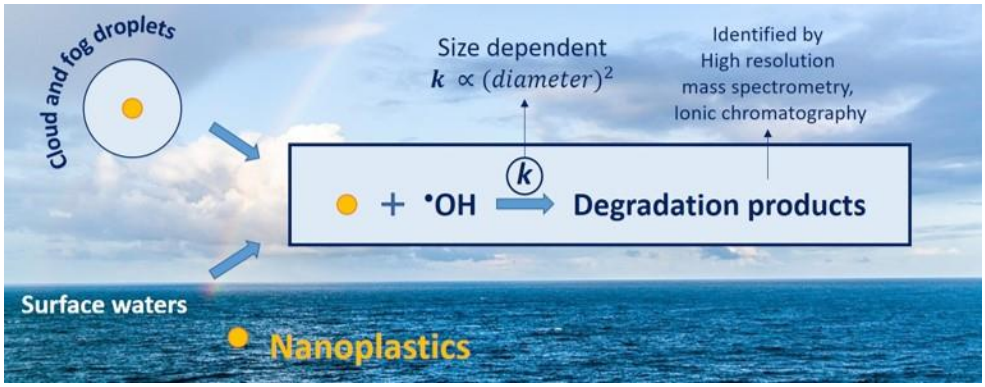

Abstract

Microplastics (MPs) and nanoplastics (NPs) are ubiquitous and contaminate soil, surface waters, atmospheric aerosol, precipitations, indoor and outdoor environments. However, the occurrence, transformation and fate of NPs in the environment are still unclear. In this work, polystyrene nanoparticles (PS-NPs) are used as a proxy of NPs to study their reactivity and potential impact on atmospheric and surface waters. In particular, the reactivity with hydroxyl radicals (•OH) in the aqueous phase is investigated. For the first time, a reactivity constant for the reaction of NPs with •OH is measured, strongly dependent on the exposed particle surface area of NPs. Degradation products (short chain carboxylic acids and aromatic compounds), obtained by direct and •OH-mediated photolysis of PS-NPs suspensions, are identified by mass spectrometry. Irradiation of a PS-NPs suspension under natural sunlight for 1 year has shown the formation of formic acid and organic compounds similar to those found in riverine and cloud dissolved organic matter, which could contribute significantly to the dissolved organic matter in the aqueous phase.

Keywords: Nanoplastics; polystyrene; hydroxyl radical; dissolved organic matter; kinetic constant.

1. Introduction

The large production of plastic material (PlasticsEurope, 2019), together with the mishandling of plastic waste, has resulted in ubiquitous plastic pollution, which now reaches even the most remote areas of the Earth (Allen et al., 2019; Bergmann et al., 2019) and has dramatic consequences on flora and fauna (Acampora et al., 2017; Todd et al., 2010). Plastics undergo a slow process of erosion in the environment, which is defined as the mass loss of the polymer matrix and is due to the loss of monomers, oligomers or even pieces of non-degraded polymer (Göpferich, 1996). This process decreases the size of plastic debris down to microplastics (MPs) and nanoplastics (NPs), defined as plastic debris with diameters between 1 µm and 5 mm and lower than 1 µm, respectively (Frias and Nash, 2019). Other possible sources of MPs and NPs are landfills or waste incineration, as well as synthetic fibers from clothes and houses (Dris et al., 2016; Liu et al., 2019).

Microplastics (MPs) contaminate soils, sediments and surface waters (both seawater and fresh waters) (Besseling et al., 2014; Scheurer and Bigalke, 2018; Yonkos et al., 2014); for example they represent 94% (in number) of collected plastic debris in the Great Pacific Garbage Patch (Lebreton et al., 2018). Recent studies have shown that MPs occur also in atmospheric aerosol and precipitations (Allen et al., 2019; Bergmann et al., 2019; Klein and Fischer, 2019), and their presence has also been documented in indoor and outdoor environments in Paris and Dongguan (Cai et al., 2017; Dris et al., 2017; Gasperi et al., 2018). In the last decades there has been a growing interest on MPs occurrence in the environment and on their potential toxicity (Anbumani and Kakkar, 2018; Dris et al., 2018; Koelmans et al., 2019), even though their environmental impact is still under debate (Backhaus and Wagner, 2019). While MPs have been measured in several environmental matrices (Chen et al., 2020; Han et al., 2019; Li et al., 2019; Xu et al., 2020), the occurrence of NPs in the environment is almost unknown (Lehner et al., 2019), mainly due to sampling and instrumental limitations (Mintenig et al., 2018; Schwaferts et al., 2019; Ter Halle et al., 2017). Up to now the occurrence, transformation, transport and fate of NPs in the environment have still been unclear. Moreover, MPs and NPs are not

68 inert and they can react and interact with chemical species that occur in the surrounding environment
69 (Jeong et al., 2018; Lee et al., 2019).
70 Erosion of MPs and NPs is the result of mechanical abrasion, oxidation, UV radiation or
71 microbiological activity (da Costa et al., 2016; Dawson et al., 2018; Lambert et al., 2013; Mattsson
72 et al., 2018). When a plastic piece degrades down to parts with sizes in the nanometre scale, the
73 exposed area increases drastically and so does the surface reactivity (Mattsson et al., 2018). However,
74 the dependence of plastics degradation kinetics upon their particle size is almost unknown, because
75 most of the degradation studies are carried out on large plastics pieces or on polymeric films (Gewert
76 et al., 2015; O'Brine and Thompson, 2010).
77 The main abiotic degradation process of plastics is photo-initiated oxidation (Gomiero, 2019),
78 which leads to polymer chain scission, branching and formation of polymer fragments as well as of
79 volatile compounds (Gewert et al., 2015). Photochemistry plays a key role in these transformation
80 processes, by direct photodegradation or by indirect photolysis, through the photogeneration of
81 reactive transient species such as the hydroxyl radical, $^{\bullet}OH$ (Calza and Vione, 2016; Faust, 1994).
82 MPs and NPs in the atmosphere and in surface waters are exposed to sunlight and oxidants (e.g.,
83 $^{\bullet}OH$). Bubble bursting and wind action can suspend MPs and NPs in air, where they could be present
84 as dry or deliquescent (in-droplet) particles. In atmospheric waters, like cloud and fog droplets, MPs
85 and NPs are even more exposed to gas and aqueous phase oxidants: for instance, the $^{\bullet}OH$ steady-state
86 concentration in cloud water is 2 orders of magnitude higher than in sea water (Lallement et al., 2018;
87 Olasehinde, 2012). Therefore, the degradation pathway(s) of MPs and NPs in atmospheric and surface
88 waters can be similar, considering that in both cases they are exposed to sunlight, gas-phase and
89 liquid-phase oxidants.
90 The objective of this work is to better understand the reactivity of an aqueous suspension of
91 polystyrene NPs (PS-NPs) in the presence of sunlight (direct photolysis) and hydroxyl radical
92 (indirect photolysis) that is a relevant oxidant in surface waters and atmospheric liquid particles. To

develop this new approach to study the reactivity of NPs in the environment, we decided to use well-defined polymeric NPs. PS standards with different monodisperse particle sizes are commercially available, and are very suitable for studying the correlation between the reactivity and the exposed surface. For the first time, a reactivity constant with $^{\bullet}OH$ is determined, which can be implemented into atmospheric and surface waters chemistry models (Bodrato and Vione, 2014) to understand the environmental impact of NPs degradation. Moreover, the identification of degradation products allows for the estimation of the contribution of NPs degradation to the natural dissolved organic matter occurring in the aqueous phase. This work can significantly contribute to assess the impact of NPs abiotic degradation in the atmospheric aqueous phase, like cloud and fog droplets, and surface waters.

2. Material and Methods

2.1. *Materials and procedures*

Suspensions (1% solids content w/w) of PS-NPs in water were purchased from Thermo Fischer Scientific (diameter of 102 ± 1 nm, 203 ± 5 nm, 400 ± 9 nm, and 600 ± 9 nm). The suspensions for irradiation were prepared daily by mixing the stock suspension of PS-NPs, previously sonicated, with MilliQ water. After irradiation and before analysis, all the suspensions were filtered on 0.22 µm nylon filters from Sigma-Aldrich. Blank experiments were carried out to verify that no organic material was released from the filter. Additional information on chemicals used are available in the Supporting Information (SI), paragraph SI-S1.

2.2. *Analysis of product formation - UVA Irradiation*

Aliquots of 15 mL of PS-NPs suspensions in Milli-Q water (0.05% solid) were irradiated in a photoreactor placed horizontally in a custom-built wood container covered with aluminium foil. The photoreactor consisted of a closed quartz tube (diameter 2.5 cm). Two UVA fluorescent lamps (Narva LT 18W/009), with emission spectrum ranging mainly from 300 to 440 nm, were placed on top of

the photoreactor (distance 6 cm), as reported in Figures S1-S2. UVA radiation was chosen because it represents the main UV fraction of solar light. PS-NPs with diameter of 400 ± 9 nm were chosen for this series of experiments, because they can be easily filtered and analysed by means of SMPS (scanning mobility particle sizer, SI-S2), in order to determine the size and concentration of the suspension and to investigate eventual formation of aggregates. All the experiments were carried out at 293 ± 2 K using a continuous flow of compressed air to cool the system. An aliquot of the suspension (3 mL) was withdrawn from the reactor and used for the analysis of degradation products at fixed times. Filtered solutions were analysed using an ElectroSpray Ionization-Differential Mobility Analyser (ESI-DMA) coupled with Atmospheric Pressure interface Time Of Flight Mass Spectrometer (Tofwerk) (ESI-DMA-APi-TOF) (Kangasluoma et al., 2016; Passananti et al., 2019). Acetate and formate anions were determined by ion chromatography. More details on the analytical methods and instrumentation are available in SI-S2. The size and the concentration of PS-NPs were measured by SMPS before and after irradiation. No difference was found: PS-NPs keep the same diameter (no aggregation) and the same concentration.

2.3. *Competition method for the measurement of the reactivity constant between PS and ˙OH.*

The reaction rate constants between ˙OH and PS-NPs were measured using the competition method described by Zhou and Mopper (1990), employing benzoic acid (hereafter BZ) as a probe. Suspensions containing 0.05% PS-NPs, 50 mM H_2O_2 and BZ with different concentrations, varying from 0.18 mM to 1.2 mM, were irradiated under UVA light for 60 minutes. In these experiments the loading of PS-NPs was kept constant, to avoid interference of varying NPs loadings on the light field and irradiance in the suspensions. In such a way, the light scattering of the suspension would not change among different experiments and would thus not affect the measured rate constants. To carry out kinetic competition, BZ concentration was thus varied. The time evolution of BZ was monitored by High-Performance Liquid Chromatography coupled with Diode Array Detection (HPLC–DAD),

using conditions detailed in SI-S3. Blank experiments excluded the degradation of BZ under UVA irradiation alone (direct photolysis).

2.4.*Experiment under real sunlight irradiation*

A suspension of PS 100 nm in MilliQ water (0.2% v/v) was exposed for 14 months (August 1st, 2018-October, 1st, 2019) on the rooftop of the Physicum building in Kumpula Campus in Helsinki (Finland). The irradiation set-up is shown in Figure S3. The average temperature during this period was 8.5°C, with a minimum on January 22nd (2019) of -18.9°C and a maximum on July 28th (2019) of 32.1°C. The suspension froze during wintertime, but the large amount of air inside the reactor prevented breaking of the glass. Filters with mesh size lower than 0.2 µm were not available, thus we filtered the 100 nm PS-NPs suspension on 0.2 µm filters by gravity, without application of pressure. The resulting solution was limpid and the particles that might have passed through the filter did not affect the following spectroscopic and spectrometric analysis. Solar radiation was measured by SMEARIII station with a time resolution of one minute, and the relevant data are available online at SMEAR website (https://avaa.tdata.fi/web/smart/smear).

3. Results and Discussion

3.1 *Interaction with hydroxyl radicals*

Surface modification due to polymers aging by light and gas-phase oxidants, such as O_3, is well known (Singh and Sharma, 2008; Yousif and Haddad, 2013). However, experiments are usually performed on films and with high concentration of O_3, which are non-representative of environmental conditions. Concerning PS, attention has been focused on the functionalisation of the polymer chain and on surface changes, using ATR/FTIR spectroscopy and microscopy techniques (SEM, AFM) (Yang et al., 2018; Zhang et al., 2000).

PS particles occurring in surface waters and in cloud/fog waters can also react with aqueous-phase oxidants, such as most notably the hydroxyl radicals (•OH) (Arakaki et al., 2013; Faust and Allen,

1993; Mopper and Zhou, 1990; Vione et al., 2010). A previous study of oxidation in dichloromethane reveals that ˙OH addition to PS occurs at the phenyl groups, and that mucondialdehydes are produced by chain scission (Weir, 1978). Surface modifications and functionalisation of MPs and NPs lead to increased hydrophilicity, which could have an effect on ice nucleating properties (Ganguly and Ariya, 2019). However, to our knowledge, no study on PS reactivity with ˙OH has been carried out in the aqueous phase. As first approach, we investigated the potential reactivity between PS-NPs and photogenerated ˙OH in aqueous solution. Figure 1 reports a preliminary test of UVA-irradiation of PS-NPs in the presence of H_2O_2 and benzoic acid (BZ) in water, using the experimental conditions detailed in SI-S4. The plot reports the BZ concentration as a function of time. The degradation rate of BZ decreases in the presence of PS-NPs, suggesting that PS-NPs may be able to significantly scavenge ˙OH.

3.2 *Reactivity of PS-NPs: measurement of the reactivity constant with hydroxyl radical*

PS-NPs react with ˙OH, but no information on the reactivity rate constants is reported in previous works. Reactivity constants are essential for modelling studies, with the aim of assessing PS-NPs degradation in different environmental scenarios as well as their ability to scavenge ˙OH and to affect photo-oxidation cycles in natural waters. For the first time, the rate constant of PS-NPs with ˙OH is determined with the competition method described in Section 2.3, using BZ as reference compound. Three different sizes of PS-NPs are used, namely 200 nm, 400 nm and 600 nm. As discussed in detail in SI-S6, the second-order kinetic constants between PS and ˙OH are calculated with the following equation:

$$k_{OH,PS} = \frac{a}{b} \times k_{OH,BZ} - [H_2O_2] \times k_{OH,H_2O_2} \quad (1)$$

where *a/b* is the ratio between the slope and the intercept of the linear correlation reported in the plot (x = inverse of BZ concentration, y = inverse of BZ degradation rate), $k_{OH,BZ}$ is the second-order reaction rate constant between BZ and ˙OH (5.9×10^9 M^{-1} s^{-1}) (Buxton et al., 1988), [H_2O_2] is the hydrogen peroxide concentration, and k_{OH,H_2O_2} is the second-order reaction rate constant between

192 •OH and H_2O_2 (2.7×10^7 M^{-1} s^{-1}) (Buxton et al., 1988). Figure S4 shows the plot used to determine
193 the kinetic constant. BZ is also a degradation product of PS-NPs (*see below*); however, due to the
194 short time of the kinetic experiments and the large concentration difference between initially added
195 and photogenerated BZ, there is no interference due to the formation of degradation products. This
196 applies both to the monitoring of the BZ time trend, and to the ability of the products (including BZ)
197 to scavenge •OH on their own. Indeed, less than 0.1% of •OH would react with BZ produced during
198 PS degradation in one hour.
199 The kinetic constants between •OH and PS-NPs ($k_{OH,PS}$) are reported in Table 1. Because the
200 concentration of PS-NPs used for the rate-constant calculation was expressed in #particles mL^{-1} (see
201 SI-S6), the measure unit of $k_{OH,PS}$ is mL s^{-1} #particles^{-1}. We observed that the size of the particles
202 (*i.e.*, their surface area) plays a role in particles reactivity, and that the values of $k_{OH,PS}$ are different
203 for each PS particle size. The kinetic constant is higher for PS 600 nm, which exposes a larger surface
204 area, and smaller for PS 200 nm, which exposes a surface area of 0.126 μm^2 per particle (see Table
205 1). This result can be explained by the fact that •OH would react with the PS surface sites (most likely,
206 the aromatic rings) and it has no access to the polymer bulk. The measured kinetic constants are
207 proportional to the square of the diameter d of the particles ($k_{OH,PS} \propto d^2$, see Figure S5); therefore,
208 the reactivity constant of PS-NPs can be expressed as a function of their diameter, allowing for the
209 extrapolation of kinetic constants at different diameters (see Table 1). We decided to express the
210 kinetic constants as a function of the diameter, in order to employ them in kinetic models in
211 combination with environmental data. Indeed, environmental data about NPs and MPs provide
212 information on their concentration (#particles/volume) and size (generally a range), without
213 specifying the surface area or the specific shape of the collected debris. Therefore, a kinetic constant
214 expressed as a function of the diameter would be more useful compared to a surface-area-normalized
215 rate constant. Further studies are needed to obtain data on the surface area of NPs in the environment,
216 in order to overcome this spherical-approximation. It is important to notice that the reactivity is higher

for single particles with larger diameters and higher surface area; however, at equal mass concentration, PS-NPs with lower particle size (200 nm) expose a higher surface area than PS-NPs with larger particle size (600 nm) and thus show higher reactivity, as reported in Figure S6 and Table S3.

3.3 *Impact of environmental stressing agents on PS-NPs: degradation products*

We have demonstrated that •OH reacts with PS-NPs and determined the reaction rate constants, but little is known about the impact of degraded plastics on the environment, in particular concerning the release of organic compounds. Vicente et al (2009) studied in detail the effect of O_3 and UVA radiation on aerosolised PS-NPs. Davidson et al. (2005) investigated the surface modification after O_3 and light exposure, and analysed the photodegradation products with GC-MS after washing with methanol or water. They found that benzaldehyde, acetophenone, BZ, carboxylic acids, aromatic ketones and esters are produced during PS exposure to O_3 and light. However, limited information is available concerning the photodegradation products formed by •OH reactions with PS-NPs. Therefore, we investigated how plastic degradation by •OH affects dissolved organic matter chemical composition. Suspensions of PS-NPs were exposed to 4 experimental conditions described in Table S1 under the irradiation set-up presented in Figure S2. This set-up allowed for estimating the impact of: (1) direct photodegradation + photogenerated •OH (indirect photolysis); (2) direct photodegradation alone; (3) reactivity with H_2O_2 in dark conditions; and (4) possible hydrolysis/degradation in dark conditions. Suspensions were sampled at fixed times, then filtered on nylon filters and analysed by ESI-DMA-APiToF. High-resolution mass spectrometry allows for the attribution of molecular formulas to degradation products. Trends of the main products formed by indirect and direct photodegradation are reported in Figure S7a and S7b, respectively, while degradation products formed by reactivity with and without H_2O_2 in dark conditions are reported in Figure S8. The •OH reactivity induces the formation of carboxylic compounds such as formic (also

241 detected as formic acid dimer), acetic, lactic acids, and aromatic acids like BZ, as well as aliphatic
242 and aromatic aldehydes like muconaldehyde and benzaldehyde.
243 Among the products of PS-NPs photodegradation, benzoquinone, dibenzoyl methane and benzoic
244 anhydride are also observed. The benzene signal increases by more than 350% of the initial value,
245 while the phenol signal increases by 40% during the first 24h and later on decreases, as shown in
246 Figure 2. The formation of degradation products could be explained through the •OH addition to π-
247 systems or hydrogen abstraction. A possible reaction mechanism, detailing the reactivity of
248 polystyrene and the formation of degradation products, is reported in Figure 3. We considered the
249 reactions induced by photogenerated •OH (light + H_2O_2), but the mechanism is probably the same
250 with light only. The tertiary polystyryl radicals, generated by hydrogen abstraction or •OH addition,
251 can efficiently react with molecular oxygen to form peroxyl radicals, ROO•. The latter can recombine
252 or give sequential reactions, leading to the formation of hydroxyl, carbonyl or carboxylic functions.
253 The carboxylic group RCOOH can react with •OH to give RCOO•, which decomposes to form R• and
254 CO_2 (Gardette et al., 1995). Tertiary polystyryl radicals can be generated by absorption of light with
255 wavelength longer than 300 nm (Gardette et al., 1995), explaining why formation of BZ,
256 benzaldehyde, benzoic anhydride, dibenzoyl methane, benzene, acetic and formic acids are also
257 observed in the case of direct photodegradation (Figure 2). However, the formation of the tertiary
258 polystyryl radicals seems to be enhanced in the presence of •OH, as suggested by the much higher
259 concentration values of photodegradation products in the H_2O_2 + light experiments compared to light
260 alone. A previous study on the irradiation of PS films in both humid and dry conditions revealed the
261 formation of acetophenone (Gardette et al., 1995). This degradation product is not detected under our
262 experimental conditions in the presence of •OH, while its signal increases during the direct photolysis
263 process (200% of the initial value). The rationale for the lack of acetophenone in the •OH experiments
264 could be that this compound reacts rapidly with •OH, with a second-order reaction rate constant of
265 6.5×10^9 $M^{-1}s^{-1}$ (Neta and Dorfman, 1968), thereby disappearing immediately after formation. Dark

experiments yield degradation products in limited amount, as reported in Figure S8 that shows the trends observed with PS-NPs and (when relevant) H_2O_2.

ESI-DMA-APiToF allows for clearly identifying the degradation products, but does not provide reliable quantification: the complexity of the matrix makes it difficult to perform signal calibration, even with standard additions. For this reason, PS-NPs suspensions subjected to experimental condition (1) (H_2O_2 + light) were analysed with ion chromatography to quantify acetic and formic acids, while benzoic acid (BZ) concentration was measured with the same HPLC method described previously. Trends and comparison with mass signals are reported in Figure S9. During the first 24h of irradiation, the concentration of acetic and formic acids increases rapidly. It then reaches 0.38 mM and 0.25 mM respectively, after 4 days of irradiation. BZ concentration increases to around 63 µM after 4 days of irradiation. The formation of these degradation products contributes to the dissolved organic carbon (DOC): acetic acid is responsible for an increase of 9.1 mgC L^{-1}, formic acid of 3.0 mgC L^{-1}, and BZ of 5.3 mgC L^{-1}. These values are of the same order of magnitude as the DOC in atmospheric hydrometeors (Bianco et al., 2015; Herckes et al., 2013, 2002; van Pinxteren et al., 2016) and in surface waters, except for the high-DOC aquatic systems (Bittar et al., 2016; Chen et al., 2004; Del Castillo et al., 1999; Galgani and Engel, 2016; Massicotte et al., 2017; Stedmon and Cory, 2014). Therefore, PS-NPs degradation could potentially impact the composition of the aqueous phase in both atmospheric and surface waters.

3.4 *Environmental conditions: PS-NPs exposed for 14 months to sunlight and temperature changes (direct photolysis)*

Laboratory irradiations give a first rapid estimate of the degradation of PS-NPs in the aqueous phase. However, longer irradiations in real environmental conditions are more suitable to investigate the release of organic compounds during PS-NPs degradation. A suspension of PS 100 nm in MilliQ water was exposed to sunlight from August 1st, 2018 to October, 1st, 2019. Figure S10 reports temperature and radiation averaged on hourly measurements for the considered period. PS-NPs were

291 degraded, they agglomerated in clusters and the aqueous system became yellowish (visual control).
292 An UV-vis spectrum after filtration was recorded showing the formation of chromophoric organic
293 compounds that absorb in the UV region up to 400 nm (Figure S11). The suspension was analysed
294 before and after solar exposure, using the same methods described for the laboratory irradiation
295 (Section 2.2). Figure S12a reports the variation in MS signals of selected compounds, while Figure
296 S12b reports the full mass spectrum obtained for the irradiated suspension. Mass spectrometric
297 analysis shows the formation of formic, benzoic and lactic acids and of benzaldehyde, while the
298 formation of other compounds is negligible. Probably, during 1-year irradiation, the degradation
299 products of PS that absorb in the near UV (see Figure S11) are transformed into small organic
300 compounds by photochemical reactions. However, Figure S12b reveals the presence of many
301 unidentified compounds, with a spectrum shape similar to those obtained for riverine and cloud
302 dissolved organic matter.(Bianco et al., 2018; Dubinenkov et al., 2015) This similarity is probably
303 due to the presence of a large variety of organic compounds, with hydroxyl, carboxylic and carbonyl
304 functions, which might be similar to the composition of natural dissolved organic matter. This
305 hypothesis is supported by the Excitation Emission Matrix (EEM) fluorescence spectrum of the liquid
306 phase (Figure S13). The presence of an emission signal around 410 nm induced by excitation around
307 300 nm recalls one of the characteristic peaks of humic substances, namely peak C (Coble, 1996) that
308 is routinely observed in surface waters (Holbrook et al., 2006). A similar peak was also observed for
309 HULIS in the atmosphere (Muller et al., 2008), and it could be due to highly oxygenated small
310 compounds (Ghigo et al., 2019) that could derive from several oxidation steps during many months
311 of sunlight exposure. Formic, acetic and benzoic acid quantification reveals concentration values of
312 7.83 mM, 4.98 mM and 0.13 mM, respectively (see Table S2), and the detected concentration of
313 formic acid corresponds to 94.0 mgC L^{-1}. Formate represents the last step of the degradation of
314 organic matter in the aqueous phase, as described in many environmental aqueous phase chemistry
315 models (Ervens, 2015; Herrmann et al., 2000; Li et al., 2017; Mouchel-Vallon et al., 2017).

4. Conclusions

This work aims at evaluating the abiotic degradation of PS-NPs in the aqueous phase, as a proxy of nanoplastics to study the reactivity with hydroxyl radicals. The results obtained can be useful for both surface and atmospheric waters, like cloud and fog droplets.

To get insight into the environmental significance of the present findings we have compared the potential effect of PS-NPs and DOC as •OH scavengers. The DOC is, indeed, the main scavenger of •OH radicals occurring in freshwater and cloud-water (Arakaki et al., 2013; Gligorovski et al., 2015). Figure 4 reports an estimate of $k_{scavenger}$ (s^{-1}) of •OH, which is the sum of the contributions of •OH reaction with DOC and NPs, as a function of the DOC ($k_{DOC} = 2\times10^4$ (L s^{-1} mgC^{-1}) × DOC) and NPs (Gligorovski et al., 2015). The typical DOC interval in cloud water (0-10 mgC L^{-1}) (Deguillaume et al., 2014; van Pinxteren et al., 2016) is highlighted in light blue in the figure, and that in surface freshwaters (> 1 mgC L^{-1}) in violet (Wetzel, 2001). Concentrations of DOC higher than 30 mgC L^{-1} are measured in surface water in specific cases only (Wetzel, 2001) but they are not considered in this work, because in such cases DOC is obviously the main scavenger of •OH radicals.

The concentration of PS-NPs in the environment is difficult to predict considering the lack of data. For this reason, we varied the PS-NPs concentration from 10^{10} #particles mL^{-1}, one order of magnitude higher than the concentration of NPs in polluted environments (10^9 #particles mL^{-1}, as per Gallego-Urrea et al., (2010)) down to 10^6 #particles mL^{-1}, a reasonable concentration for lesser polluted aqueous media (Gallego-Urrea et al., 2010). We considered a reactivity constant between •OH and NPs of 1.93×10^{-4} mL s^{-1} $\#particles^{-1}$, the one determined for PS-NPs 600 nm in this work. Figure 4 shows that when the DOC concentration is low, like in DOC-poor surface freshwater and atmospheric cloud-water, there is potential for NPs to significantly scavenge •OH. In particular, at 10^9 particles mL^{-1} NPs could even become the main •OH scavenger if DOC < 9 mgC L^{-1}. Moreover, at very low DOC values (1 mgC L^{-1} or below) the organic compounds released by NPs

photodegradation, especially if the latter takes place over a long time period, could give a non-negligible contribution to both the water DOC and the •OH scavenging ability.

The comparison in the reactivity of NPs and DOC suggests three main issues:

(i) The ability of NPs to scavenge •OH should be taken into account in models aimed at describing the role of •OH in environmental waters. To do so, however, additional data are needed on the •OH reactivity of other plastic types (e.g., polyethylene and polypropylene), on the correlation between size of particles and reactivity, and on the concentration of NPs in a wide variety of aquatic environments.

(ii) Due to their scavenging ability, it is very important to assess the fate of NPs upon •OH reaction, including the potential to release dissolved organic compounds.

(iii) There is also the need to compare the •OH scavenging ability of NPs themselves with that of the compounds that are released by their photodegradation, especially over long irradiation times.

In aquatic environments with higher concentration of DOC (or other •OH scavengers, such as bromide in seawater) (Buxton et al., 1988; Gligorovski et al., 2015), PS-NPs can react with sunlight as shown through direct photolysis experiments, leading to the formation of very similar degradation products as those obtained under •OH-mediated degradation. The identification of degradation products of PS-NPs suspensions subjected to direct photolysis and •OH-induced degradation highlights the formation of several compounds, mainly small carboxylic acids and some toxic compounds like benzene and phenol. These compounds could have an effect on the ecosystems by increasing the dissolved organic matter amount. Moreover, the production of light-absorbing species (Figure S11) could interfere with the natural photochemical equilibrium in environmental waters.

Our results can be implemented in models, allowing for the estimation of the amount of organic matter produced by NPs abiotic degradation and, therefore, of the impact of NPs on environmental equilibria.

Declaration of Competing Interest

The authors declare that they have no known competing financial interests or personal relationships that could have appeared to influence the work reported in this paper.

Acknowledgments

We acknowledge funding from the University of Helsinki (Three-Year Research Grants), the ERC Projects 692891-DAMOCLES and 638703-COALA, ATMATH Project.

Author contribution

A.B. formal analysis and writing-original draft, F.S. formal analysis and writing-review and editing, M.E. supervision and writing-review and editing, D.V. software, supervision and writing-review and editing, M.P. conceptualization, funding, formal analysis, writing-original draft and review.

Appendix A. Supplementary data

Supplementary data to this article can be found online.

TABLES

Diameter of PS-NPs (μm)	Particle surface area (μm^2)	$k_{OH,PS}$ (mL s^{-1} #particles^{-1})
0.20	0.126	$(6.50 \pm 0.38) \times 10^{-5}$
0.40	0.502	$(8.64 \pm 1.30) \times 10^{-5}$
0.60	1.130	$(1.93 \pm 0.22) \times 10^{-4}$
Correlation between $k_{OH,PS}$ (mL s^{-1} #particles^{-1}) and diameter of PS-NPs		
$\boldsymbol{k_{OH,PS} = (5.47 \pm 0.78) \times 10^{-4}\ d^2}$		
d = diameter (μm)		

Table 1: Kinetic constants between •OH and PS-NPs ($k_{OH,PS}$) as a function of the particle surface area for each PS-NPs size (200 nm, 400 nm and 600 nm). Correlation between $k_{OH,PS}$ and the diameter of PS-NPs. The error bounds represent the sigma-level variability derived from data fit, which was used to obtain the relevant rate constant values.

FIGURES

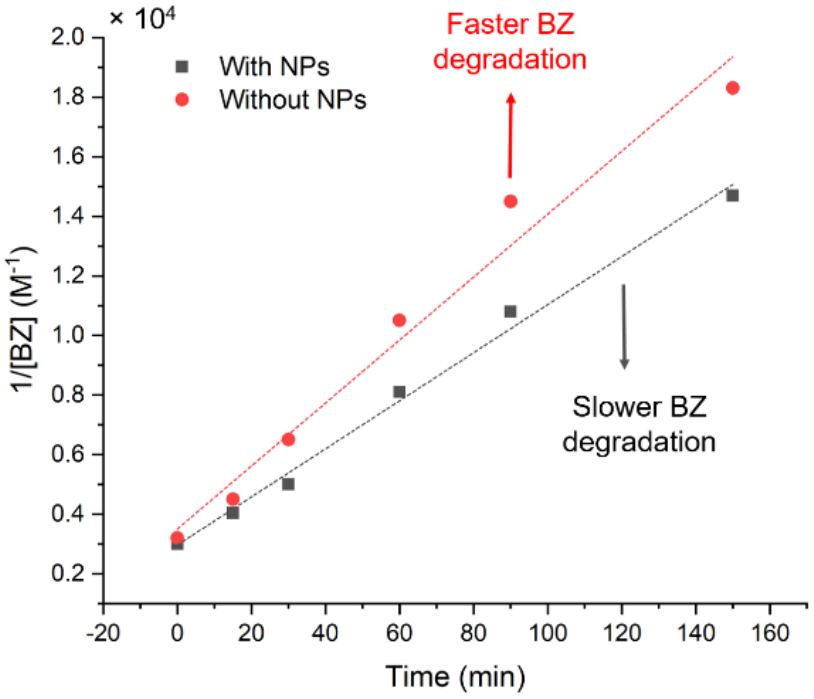

Figure 1: Degradation of BZ (expressed as 1/[BZ]) as function of time with and without NPs in the presence of 50 mM of H_2O_2 under UVA irradiation in water.

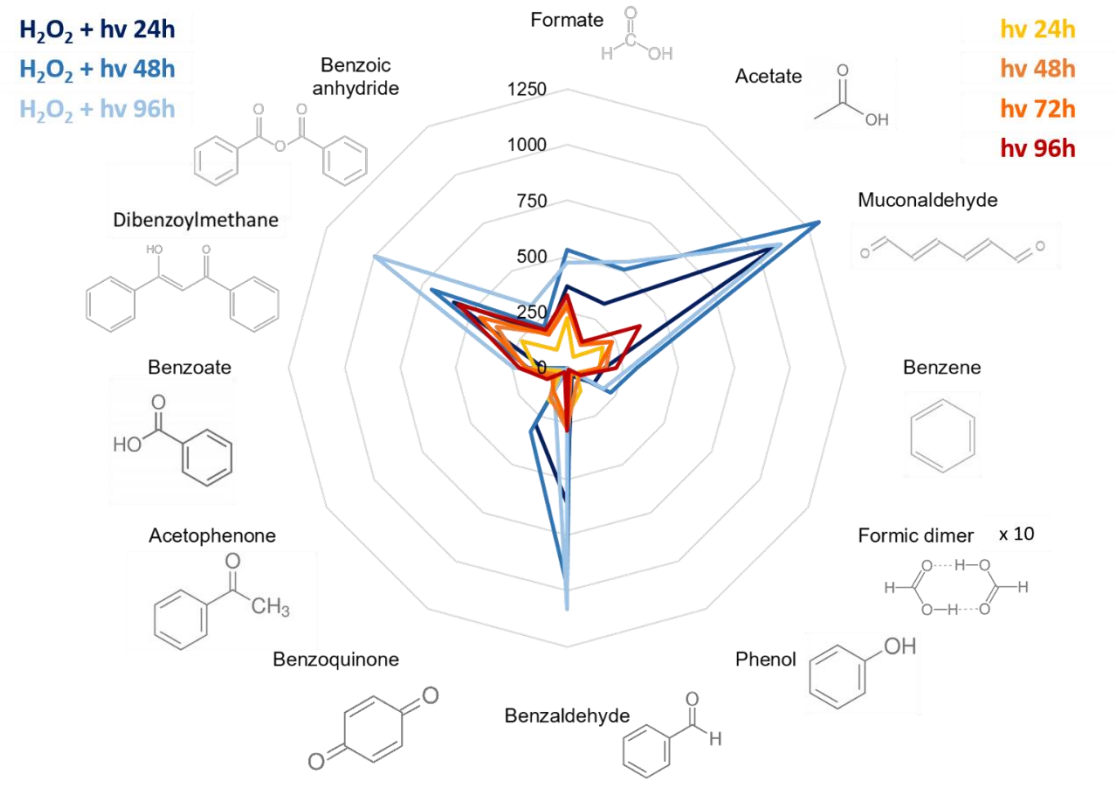

389

390 **Figure 2**: Signal increase (%) of degradation products over time under: direct photolysis + hydroxyl radical mediated

391 oxidation (H_2O_2 + hν) (in shade of blue) and b) direct photolysis (hν) (in shade of red).

392

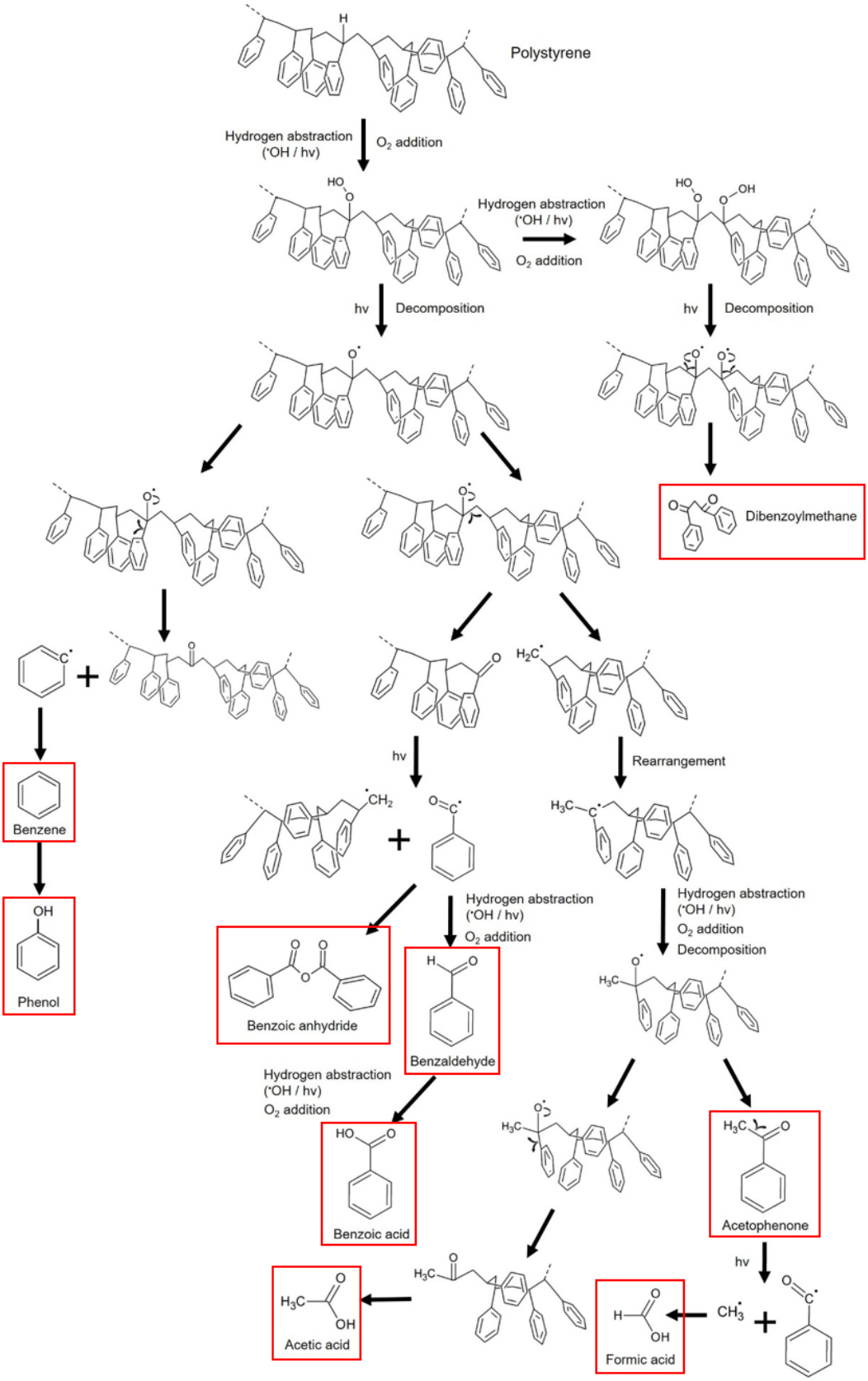

393

394 **Figure 3**: Proposed mechanism of degradation of PS with light and photogenerated hydroxyl radicals. Identified

395 compounds are framed in red.

396

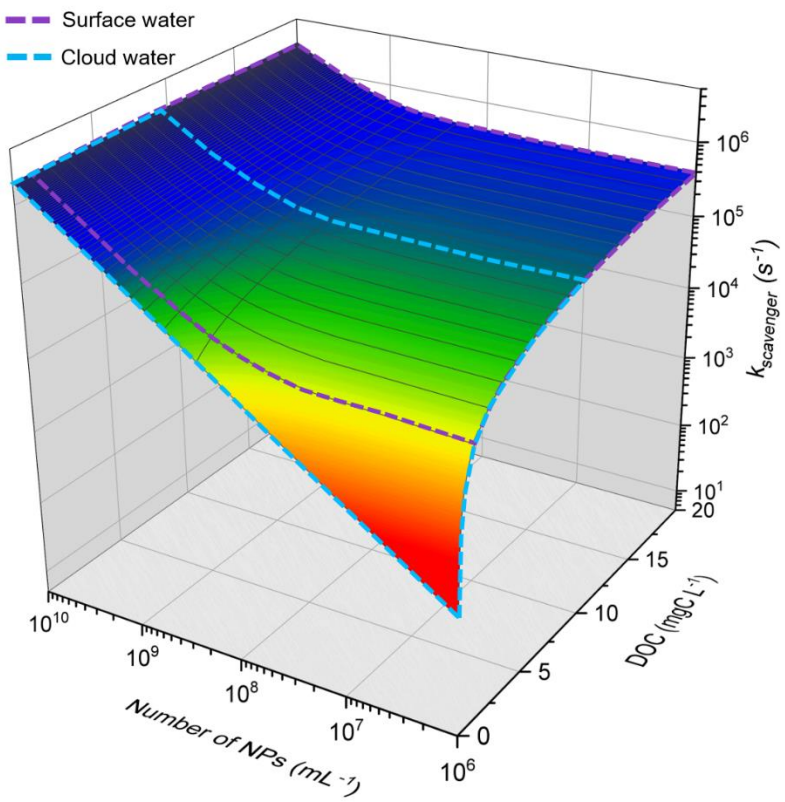

397

398 **Figure 4**: Estimated rate constants (k_{scav}) for the scavenging of •OH by PS-NPs and DOC. DOC concentration is
399 representative of surface waters (higher than 1 mgC L^{-1}), depicted in the violet interval, and of cloud water (0-10 mgC
400 L^{-1}), in light blue.

401

References

Acampora, H., Berrow, S., Newton, S., O'Connor, I., 2017. Presence of plastic litter in pellets from Great Cormorant (Phalacrocorax carbo) in Ireland. Mar. Pollut. Bull. 117, 512–514. https://doi.org/10.1016/j.marpolbul.2017.02.015

Allen, S., Allen, D., Phoenix, V.R., Le Roux, G., Durántez Jiménez, P., Simonneau, A., Binet, S., Galop, D., 2019. Atmospheric transport and deposition of microplastics in a remote mountain catchment. Nat. Geosci. 12, 339–344. https://doi.org/10.1038/s41561-019-0335-5

Anbumani, S., Kakkar, P., 2018. Ecotoxicological effects of microplastics on biota: a review. Environ. Sci. Pollut. R. 25, 14373–14396. https://doi.org/10.1007/s11356-018-1999-x

Arakaki, T., Anastasio, C., Kuroki, Y., Nakajima, H., Okada, K., Kotani, Y., Handa, D., Azechi, S., Kimura, T., Tsuhako, A., Miyagi, Y., 2013. A general scavenging rate constant for reaction of hydroxyl radical with organic carbon in atmospheric waters. Environ. Sci. Tech. 47, 8196–8203. https://doi.org/10.1021/es401927b

Backhaus, T., Wagner, M., 2019. Microplastics in the Environment: Much Ado about Nothing? A Debate. Global Challenges 1900022. https://doi.org/10.1002/gch2.201900022

Bergmann, M., Mützel, S., Primpke, S., Tekman, M.B., Trachsel, J., Gerdts, G., 2019. White and wonderful? Microplastics prevail in snow from the Alps to the Arctic. Sci. Adv. 5, eaax1157. https://doi.org/10.1126/sciadv.aax1157

Besseling, E., Wang, B., Lürling, M., Koelmans, A.A., 2014. Nanoplastic affects growth of *S. obliquus* and reproduction of *D. magna*. Environ. Sci. Technol. 48, 12336–12343. https://doi.org/10.1021/es503001d

Bianco, A., Deguillaume, L., Vaïtilingom, M., Nicol, E., Baray, J.-L., Chaumerliac, N., Bridoux, M.C., 2018. Molecular characterization of cloud water samples collected at the puy de Dôme (France) by Fourier Transform Ion Cyclotron Resonance Mass Spectrometry. Environ. Sci. Tech.. https://doi.org/10.1021/acs.est.8b01964

Bianco, A., Passananti, M., Perroux, H., Voyard, G., Mouchel-Vallon, C., Chaumerliac, N., Mailhot, G., Deguillaume, L., Brigante, M., 2015. A better understanding of hydroxyl radical photochemical sources in cloud waters collected at the puy de Dôme station – experimental versus modelled formation rates. Atmos. Chem. Phys. 15, 9191–9202. https://doi.org/10.5194/acp-15-9191-2015

Bittar, T.B., Berger, S.A., Birsa, L.M., Walters, T.L., Thompson, M.E., Spencer, R.G., Mann, E.L., Stubbins, A., Frischer, M.E., Brandes, J.A., 2016. Seasonal dynamics of dissolved, particulate and microbial components of a tidal saltmarsh-dominated estuary under contrasting levels of freshwater discharge. Estuar. Coast. Shelf. S. 182, 72–85. https://doi.org/10.1016/j.ecss.2016.08.046

Bodrato, M., Vione, D., 2014. APEX (Aqueous Photochemistry of Environmentally occurring Xenobiotics): a free software tool to predict the kinetics of photochemical processes in surface waters. Environ. Sci.: Processes Impacts 16, 732–740. https://doi.org/10.1039/C3EM00541K

Buxton, G.V., Greenstock, C.L., Helman, W.P., Ross, A.B., 1988. Critical review of rate constants for reactions of hydrated electrons, hydrogen atoms and hydroxyl radicals (•OH/•O− in aqueous solution. J. Phys. Chem. Ref. Data 17, 513–886. https://doi.org/10.1063/1.555805

441 Cai, L., Wang, J., Peng, J., Tan, Z., Zhan, Z., Tan, X., Chen, Q., 2017. Characteristic of microplastics
442 in the atmospheric fallout from Dongguan city, China: preliminary research and first evidence.
443 Environ. Sci. Pollut. R. 24, 24928–24935. https://doi.org/10.1007/s11356-017-0116-x

444 Calza, P., Vione, D., 2016. Surface Water Photochemistry, Comprehensive Series in Photochemical
445 & Photobiological Sciences. The Royal Society of Chemistry.
446 https://doi.org/10.1039/9781782622154

447 Chen, G., Feng, Q., Wang, J., 2020. Mini-review of microplastics in the atmosphere and their risks
448 to humans. Sci. Total Environ. 703, 135504. https://doi.org/10.1016/j.scitotenv.2019.135504

449 Chen, R.F., Bissett, P., Coble, P., Conmy, R., Gardner, G.B., Moran, M.A., Wang, X., Wells, M.L.,
450 Whelan, P., Zepp, R.G., 2004. Chromophoric dissolved organic matter (CDOM) source
451 characterization in the Louisiana Bight. Mar. Chem. 89, 257–272.
452 https://doi.org/10.1016/j.marchem.2004.03.017

453 Coble, P.G., 1996. Characterization of marine and terrestrial DOM in seawater using excitation-
454 emission matrix spectroscopy. Mar. Chem. 51, 325–346. https://doi.org/10.1016/0304-
455 4203(95)00062-3

456 da Costa, J.P., Santos, P.S., Duarte, A.C., Rocha-Santos, T., 2016. (Nano) plastics in the
457 environment–sources, fates and effects. Sci. Total Environ. 566, 15–26.
458 https://doi.org/10.1016/j.scitotenv.2016.05.041

459 Davidson, M.R., Mitchell, S.A., Bradley, R.H., 2005. Surface studies of low molecular weight
460 photolysis products from UV-ozone oxidised polystyrene. Surf. Sci. 581, 169–177.
461 https://doi.org/10.1016/j.susc.2005.02.049

462 Dawson, A.L., Kawaguchi, S., King, C.K., Townsend, K.A., King, R., Huston, W.M., Nash, S.M.B.,
463 2018. Turning microplastics into nanoplastics through digestive fragmentation by Antarctic krill. Nat.
464 Commun. 9, 1001. https://doi.org/10.1038/s41467-018-03465-9

465 Deguillaume, L., Charbouillot, T., Joly, M., Vaïtilingom, M., Parazols, M., Marinoni, A., Amato, P.,
466 Delort, A.-M., Vinatier, V., Flossmann, A., Chaumerliac, N., Pichon, J.M., Houdier, S., Laj, P.,
467 Sellegri, K., Colomb, A., Brigante, M., Mailhot, G., 2014. Classification of clouds sampled at the puy
468 de Dôme (France) based on 10 yr of monitoring of their physicochemical properties. Atmos. Chem.
469 Phys. 14, 1485–1506. https://doi.org/10.5194/acp-14-1485-2014

470 Del Castillo, C.E., Coble, P.G., Morell, J.M., Lopez, J.M., Corredor, J.E., 1999. Analysis of the
471 optical properties of the Orinoco River plume by absorption and fluorescence spectroscopy. Mar.
472 Chem. 66, 35–51. https://doi.org/10.1016/S0304-4203(99)00023-7

473 Dris, R., Gasperi, J., Mirande, C., Mandin, C., Guerrouache, M., Langlois, V., Tassin, B., 2017. A
474 first overview of textile fibers, including microplastics, in indoor and outdoor environments. Environ.
475 Pollut. 221, 453–458. https://doi.org/10.1016/j.envpol.2016.12.013

476 Dris, R., Gasperi, J., Rocher, V., Tassin, B., 2018. Synthetic and non-synthetic anthropogenic fibers
477 in a river under the impact of Paris Megacity: Sampling methodological aspects and flux estimations.
478 Sci. Total Environ. 618, 157–164. https://doi.org/10.1016/j.scitotenv.2017.11.009

479 Dris, R., Gasperi, J., Saad, M., Mirande, C., Tassin, B., 2016. Synthetic fibers in atmospheric fallout:
480 a source of microplastics in the environment? Mar. Pollut. Bull. 104, 290–293.
481 https://doi.org/10.1016/j.marpolbul.2016.01.006

Dubinenkov, I., Flerus, R., Schmitt-Kopplin, P., Kattner, G., Koch, B.P., 2015. Origin-specific molecular signatures of dissolved organic matter in the Lena Delta. Biogeochemistry 123, 1–14. https://doi.org/10.1007/s10533-014-0049-0

Ervens, B., 2015. Modeling the processing of aerosol and trace gases in clouds and fogs. Chem. Rev. 115, 4157–4198. https://doi.org/10.1021/cr5005887

Faust, B.C., 1994. Photochemistry of clouds, fogs, and aerosols. Environ. Sci. Tech. 28, 216A-222A. https://doi.org/10.1021/es00054a001

Faust, B.C., Allen, J.M., 1993. Aqueous-phase photochemical formation of hydroxyl radical in authentic cloudwaters and fogwaters. Environ. Sci. Tech. 27, 1221–1224. https://doi.org/10.1021/es00043a024

Frias, J., Nash, R., 2019. Microplastics: Finding a consensus on the definition. Mar. Pollut. Bull. 138, 145–147. https://doi.org/10.1016/j.marpolbul.2018.11.022

Galgani, L., Engel, A., 2016. Changes in optical characteristics of surface microlayers hint to photochemically and microbially mediated DOM turnover in the upwelling region off the coast of Peru. Biogeosciences 13, 2453–2473. https://doi.org/10.5194/bg-13-2453-2016

Gallego-Urrea, J.A., Tuoriniemi, J., Pallander, T., Hassellöv, M., 2010. Measurements of nanoparticle number concentrations and size distributions in contrasting aquatic environments using nanoparticle tracking analysis. Environ. Chem. 7, 67. https://doi.org/10.1071/EN09114

Ganguly, M., Ariya, P.A., 2019. Ice nucleation of model nanoplastics and microplastics: a novel synthetic protocol and the influence of particle capping at diverse atmospheric environments. ACS Earth Space Chem. 3, 1729–1739. https://doi.org/10.1021/acsearthspacechem.9b00132

Gardette, J.-L., Mailhot, B., Lemaire, J., 1995. Photooxidation mechanisms of styrenic polymers. Polym. Degrad. Stabil., 48(3), 457–470. https://doi.org/10.1016/0141-3910(95)00113-Z

Gasperi, J., Wright, S.L., Dris, R., Collard, F., Mandin, C., Guerrouache, M., Langlois, V., Kelly, F.J., Tassin, B., 2018. Microplastics in air: are we breathing it in? Current Opinion in Environmental Science & Health 1, 1–5. https://doi.org/10.1016/j.coesh.2017.10.002

Gewert, B., Plassmann, M.M., MacLeod, M., 2015. Pathways for degradation of plastic polymers floating in the marine environment. Environ. Sci.: Processes Impacts 17, 1513–1521. https://doi.org/10.1039/C5EM00207A

Ghigo, G., Vione, D., Berto, S., 2019. Experimental and theoretical study of the fluorescence emission of ferulic acid: Possible insights into the fluorescence properties of humic substances. Spectrochim. Acta A 117587. https://doi.org/10.1016/j.saa.2019.117587

Gligorovski, S., Strekowski, R., Barbati, S., Vione, D., 2015. Environmental Implications of Hydroxyl Radicals (•OH). Chem. Rev. 115, 13051–13092. https://doi.org/10.1021/cr500310b

Gomiero, A. (Ed.), 2019. Plastics in the Environment. IntechOpen. https://doi.org/10.5772/intechopen.75849

Göpferich, A., 1996. Mechanisms of polymer degradation and erosion. Biomaterials 17, 103–114. https://doi.org/10.1016/0142-9612(96)85755-3

Han, M., Niu, X., Tang, M., Zhang, B.-T., Wang, G., Yue, W., Kong, X., Zhu, J., 2019. Distribution of microplastics in surface water of the lower Yellow River near estuary. Sci. Total Environ. 135601. https://doi.org/10.1016/j.scitotenv.2019.135601

Herckes, P., Lee, T., Trenary, L., Kang, G., Chang, H., Collett, J.L., 2002. Organic matter in central California radiation fogs. Environ. Sci. Tech. 36, 4777–4782. https://doi.org/10.1021/es025889t

Herckes, P., Valsaraj, K.T., Collett, J.L., 2013. A review of observations of organic matter in fogs and clouds: Origin, processing and fate. Atmos. Res. 132–133, 434–449. https://doi.org/10.1016/j.atmosres.2013.06.005

Herrmann, H., Ervens, B., Jacobi, H.-W., Wolke, R., Nowacki, P., Zellner, R., 2000. CAPRAM2.3: A chemical aqueous phase radical mechanism for tropospheric chemistry. J. Atmos. Chem. 36, 231–284. https://doi.org/10.1023/A:1006318622743

Holbrook, R.D., Yen, J.H., Grizzard, T.J., 2006. Characterizing natural organic material from the Occoquan Watershed (Northern Virginia, US) using fluorescence spectroscopy and PARAFAC. Sci. Total Environ. 361, 249–266. https://doi.org/10.1016/j.scitotenv.2005.11.020

Jeong, C.-B., Kang, H.-M., Lee, Y.H., Kim, M.-S., Lee, Jin-Sol, Seo, J.S., Wang, M., Lee, Jae-Seong, 2018. Nanoplastic ingestion enhances toxicity of persistent organic pollutants (POPs) in the Monogonont Rotifer Brachionus koreanus via multixenobiotic resistance (MXR) disruption. Environ. Sci. Technol. 52, 11411–11418. https://doi.org/10.1021/acs.est.8b03211

Kangasluoma, J., Attoui, M., Korhonen, F., Ahonen, L., Siivola, E., Petäjä, T., 2016. Characterization of a Herrmann-type high-resolution differential mobility analyzer. Aerosol Sci. Tech. 50, 222–229. https://doi.org/10.1080/02786826.2016.1142065

Klein, M., Fischer, E.K., 2019. Microplastic abundance in atmospheric deposition within the Metropolitan area of Hamburg, Germany. Sci. Total Environ. 685, 96–103. https://doi.org/10.1016/j.scitotenv.2019.05.405

Koelmans, A.A., Mohamed Nor, N.H., Hermsen, E., Kooi, M., Mintenig, S.M., De France, J., 2019. Microplastics in freshwaters and drinking water: Critical review and assessment of data quality. Water Res. 155, 410–422. https://doi.org/10.1016/j.watres.2019.02.054

Lallement, A., Vinatier, V., Brigante, M., Deguillaume, L., Delort, A.M., Mailhot, G., 2018. First evaluation of the effect of microorganisms on steady state hydroxyl radical concentrations in atmospheric waters. Chemosphere 212, 715–722. https://doi.org/10.1016/j.chemosphere.2018.08.128

Lambert, S., Sinclair, C.J., Bradley, E.L., Boxall, A.B., 2013. Effects of environmental conditions on latex degradation in aquatic systems. Sci. Total Environ. 447, 225–234. https://doi.org/10.1016/j.scitotenv.2012.12.067

Lebreton, L., Slat, B., Ferrari, F., Sainte-Rose, B., Aitken, J., Marthouse, R., Hajbane, S., Cunsolo, S., Schwarz, A., Levivier, A., 2018. Evidence that the Great Pacific Garbage Patch is rapidly accumulating plastic. Sci. Rep. 8, 4666. https://doi.org/10.1038/s41598-018-22939-w

Lee, W.S., Cho, H.-J., Kim, E., Huh, Y.H., Kim, H.-J., Kim, B., Kang, T., Lee, J.-S., Jeong, J., 2019. Bioaccumulation of polystyrene nanoplastics and their effect on the toxicity of Au ions in zebrafish embryos. Nanoscale 11, 3173–3185. https://doi.org/10.1039/C8NR09321K

Lehner, R., Weder, C., Petri-Fink, A., Rothen-Rutishauser, B., 2019. Emergence of nanoplastic in the environment and possible impact on human health. Environ. Sci. Technol. 53, 1748–1765. https://doi.org/10.1021/acs.est.8b05512

Li, C., Busquets, R., Campos, L.C., 2019. Assessment of microplastics in freshwater systems: A review. Sci. Total Environ. 135578. https://doi.org/10.1016/j.scitotenv.2019.135578

Li, Y., Barth, M.C., Patton, E.G., Steiner, A.L., 2017. Impact of In-Cloud Aqueous Processes on the Chemistry and Transport of Biogenic Volatile Organic Compounds: Impact of In-Cloud Processes on BVOC. J. Geophys. Res. Atmos. 122, 11,131-11,153. https://doi.org/10.1002/2017JD026688

Liu, K., Wu, T., Wang, X., Song, Z., Zong, C., Wei, N., Li, D., 2019. Consistent Transport of Terrestrial Microplastics to the Ocean through Atmosphere. Environ. Sci. Technol. 53, 10612–10619. https://doi.org/10.1021/acs.est.9b03427

Massicotte, P., Asmala, E., Stedmon, C., Markager, S., 2017. Global distribution of dissolved organic matter along the aquatic continuum: Across rivers, lakes and oceans. Sci. Total Environ. 609, 180–191. https://doi.org/10.1016/j.scitotenv.2017.07.076

Mattsson, K., Jocic, S., Doverbratt, I., Hansson, L.-A., 2018. Nanoplastics in the aquatic environment, in: Microplastic Contamination in Aquatic Environments. Elsevier, pp. 379–399. https://doi.org/10.1016/B978-0-12-813747-5.00013-8

Mintenig, S.M., Bäuerlein, P.S., Koelmans, A.A., Dekker, S.C., van Wezel, A.P., 2018. Closing the gap between small and smaller: towards a framework to analyse nano- and microplastics in aqueous environmental samples. Environ. Sci.: Nano 5, 1640–1649. https://doi.org/10.1039/C8EN00186C

Mopper, K., Zhou, X., 1990. Hydroxyl radical photoproduction in the sea and its potential impact on marine processes. Science 250, 661–664. https://doi.org/10.1126/science.250.4981.661

Mouchel-Vallon, C., Deguillaume, L., Monod, A., Perroux, H., Rose, C., Ghigo, G., Long, Y., Leriche, M., Aumont, B., Patryl, L., Armand, P., Chaumerliac, N., 2017. CLEPS 1.0: A new protocol for cloud aqueous phase oxidation of VOC mechanisms. Geosci. Model Dev. 10, 1339–1362. https://doi.org/10.5194/gmd-10-1339-2017

Muller, C.L., Baker, A., Hutchinson, R., Fairchild, I.J., Kidd, C., 2008. Analysis of rainwater dissolved organic carbon compounds using fluorescence spectrophotometry. Atmos. Environ. 42, 8036–8045. https://doi.org/10.1016/j.atmosenv.2008.06.042

Neta, P., Dorfman, L.M., 1968. Pulse radiolysis studies. XIII. Rate constants for the reaction of hydroxyl radicals with aromatic compounds in aqueous solutions, Radiation Chem. 81, 222–230. https://doi.org/10.1021/ba-1968-0081.ch015

O'Brine, T., Thompson, R.C., 2010. Degradation of plastic carrier bags in the marine environment. Mar. Pollut. Bull. 60, 2279–2283. https://doi.org/10.1016/j.marpolbul.2010.08.005

Olasehinde, E.F., 2012. Determination of hydroxyl radical in Seto inland sea and its potential to degrade irgarol. IOSRJAC 1, 07–14. https://doi.org/10.9790/5736-0150714

Passananti, M., Zapadinsky, E., Zanca, T., Kangasluoma, J., Myllys, N., Rissanen, M.P., Kurtén, T., Ehn, M., Attoui, M., Vehkamäki, H., 2019. How well can we predict cluster fragmentation inside a mass spectrometer? Chem. Commun. 55, 5946–5949. https://doi.org/10.1039/C9CC02896J

PlasticsEurope, 2019. Plastics the facts - 2018. Retrieved from https://www.plasticseurope.org/en/resources/publications/619-plastics-facts-2018

Scheurer, M., Bigalke, M., 2018. Microplastics in Swiss floodplain soils. Environ. Sci. Technol. 52, 3591–3598. https://doi.org/10.1021/acs.est.7b06003

Schwaferts, C., Niessner, R., Elsner, M., Ivleva, N.P., 2019. Methods for the analysis of submicrometer- and nanoplastic particles in the environment. TrAC Trend Anal. Chem. 112, 52–65. https://doi.org/10.1016/j.trac.2018.12.014

Singh, B., Sharma, N., 2008. Mechanistic implications of plastic degradation. Polym. Degrad. Stabil. 93, 561–584. https://doi.org/10.1016/j.polymdegradstab.2007.11.008

Stedmon, C.A., Cory, R.M., 2014. Biological origins and fate of fluorescent dissolved organic matter in aquatic environments. Aquatic organic matter fluorescence 278–299. https://doi.org/10.1017/CBO9781139045452.013

Ter Halle, A., Jeanneau, L., Martignac, M., Jardé, E., Pedrono, B., Brach, L., Gigault, J., 2017. Nanoplastic in the North Atlantic Subtropical Gyre. Environ. Sci. Technol. 51, 23, 13689-13697.

Todd, P.A., Ong, X., Chou, L.M., 2010. Impacts of pollution on marine life in Southeast Asia. Biodivers. Conserv. 19, 1063–1082. https://doi.org/10.1007/s10531-010-9778-0

van Pinxteren, D., Fomba, K.W., Mertes, S., Müller, K., Spindler, G., Schneider, J., Lee, T., Collett, J.L., Herrmann, H., 2016. Cloud water composition during HCCT-2010: Scavenging efficiencies, solute concentrations, and droplet size dependence of inorganic ions and dissolved organic carbon. Atmos. Chem. Phys. 16, 3185–3205. https://doi.org/10.5194/acp-16-3185-2016

Vicente, J.S., Gejo, J.L., Rothenbacher, S., Sarojiniamma, S., Gogritchiani, E., Wörner, M., Kasper, G., Braun, A.M., 2009. Oxidation of polystyrene aerosols by VUV-photolysis and/or ozone. Photochem. Photobiol. Sci. 8, 944. https://doi.org/10.1039/b902749a

Vione, D., Bagnus, D., Maurino, V., Minero, C., 2010. Quantification of singlet oxygen and hydroxyl radicals upon UV irradiation of surface water. Environ. Chem. Lett. 8, 193–198. https://doi.org/10.1007/s10311-009-0208-z

Weir, N.A., 1978. Reactions of hydroxyl radicals with polystyrene. Eur. Polym. J. 14, 9–14. https://doi.org/10.1016/0014-3057(78)90144-1

Wetzel, R.G., 2001. Limnology: lake and river ecosystems. gulf professional publishing.

Xu, S., Ma, J., Ji, R., Pan, K., Miao, A.-J., 2020. Microplastics in aquatic environments: Occurrence, accumulation, and biological effects. Sci. Total Environ. 703, 134699. https://doi.org/10.1016/j.scitotenv.2019.134699

Yang, R., He, Q., Wang, C., Sun, S., 2018. Surface modification of polystyrene microsphere using ozone treatment. Ferroelectrics 530, 130–135. https://doi.org/10.1080/00150193.2018.1453200

Yonkos, L.T., Friedel, E.A., Perez-Reyes, A.C., Ghosal, S., Arthur, C.D., 2014. Microplastics in four estuarine rivers in the Chesapeake Bay, U.S.A. Environ. Sci. Technol. 48, 14195–14202. https://doi.org/10.1021/es5036317

Yousif, E., Haddad, R., 2013. Photodegradation and photostabilization of polymers, especially polystyrene: review. SpringerPlus 2, 398. https://doi.org/10.1186/2193-1801-2-398

638 Zhang, D., Dougal, S., Yeganeh, M., 2000. Effects of UV irradiation and plasma treatment on a
639 polystyrene surface studied by IR− visible sum frequency generation spectroscopy. Langmuir 16,
640 4528–4532. https://doi.org/10.1021/la991353i

641 Zhou, X., Mopper, K., 1990. Determination of photochemically produced hydroxyl radicals in
642 seawater and freshwater. Mar. Chem. 30, 71–88. https://doi.org/10.1016/0304-4203(90)90062-H